Heliyon 5 (2019) e01750

Contents lists available at ScienceDirect

Heliyon

journal homepage: www.heliyon.com

Green synthesis of zero valent iron nanoparticle using mango peel extract and surface characterization using XPS and GC-MS

Biruck Desalegn *, Mallavarapu Megharaj, Zuliang Chen, Ravi Naidu

Global Centre for Environmental Remediation (GCER), Faculty of Science and Information Technology, The University of Newcastle, Callaghan, NSW2308, Australia

ARTICLE INFO

Keywords:
Environmental science
Materials chemistry
Nanotechnology
Materials science

ABSTRACT

In this study, a novel form of zero valent iron nanoparticle (GMP-nZVI) was successfully synthesized using mango peel extracts. Iron on the surface of the synthesized particle was negligible. Surface structure and compositional analysis was carried out using XPS and FTIR whereby the characteristic feature of the analysis highlighted the role of few organic compounds in the synthesis of GMP-nZVI. Depth profiling of GMP-nZVI by XPS indicated increasing intensity of Fe0 while the portion of Fe+2/Fe+3 and the dominant species which were on the surface (i.e. C and O) were decreasing. The structural form of GMP-nZVI has a layer of polyphenol followed by the oxides and hydroxides of iron onto the metallic iron which has a shell structure of 'Fe+3/Fe+2-polyphenol' complex islands on the core metallic iron (graphical abstract). The use of mango peel in the synthesis is a low cost approach and economically viable which also provides new insight of waste recycling and nanoremediation.

1. Introduction

Nano-zero valent iron (nZVI) synthesized via chemical approach has drawbacks including the use of toxic and very expensive chemical substances such as NHB4, organic solvents, stabilizing and dispersing agents [1, 2, 3, 4, 5, 6, 7, 8, 9]. Moreover, these materials when not stabilized have practical difficulties due to particle immobilization, agglomeration, the possible adherence to soil or organic particles and passivation effects via oxidative loss [10, 11, 12, 13]. Therefore, the development of clean, biocompatible, non-toxic and ecofriendly methods for synthesizing nanoparticles is required. Green synthesis of nanoparticles using naturally occurring reagents such as plant extracts as reducing and capping agents has a potential application in nanotechnology. It is superior to other methods because it is simple, cost-effective, relatively reproducible and often results in more stable materials [14].

Recently, considerable studies have been devoted to using plant extracts. Synthesis of nZVI using plant extracts of high polyphenol content have been reported by VeruTEK and the US EPA [9, 15, 16, 17]. The approach is a green route and far more efficient than the traditional production method due to the decrease in agglomerate size and enhanced mobility of the particles in applications such as for ground water remediation. An important application of stabilized nZVI via green synthesis is the treatment efficiency compared to unstabilized nanoparticles where the support could promote particle stability in aqueous suspensions and enhance reactive surfaces available for contaminant degradation [18]. Moreover, such a biological route of synthesis is assumed to be promising since its applications may leave smaller footprints and with greater environmental compatibility.

Given the increasing interest evaluating the potential environmental application of green synthesized nZVI, few studies indicated that plant based synthesis of iron nanoparticle may not be promising for the synthesis of nZVI [19, 20, 21]. Wang [19] proposed a structure of iron-polyphenol complex with ferric ion core formation. Few studies demonstrated the iron reducing ability of oxidants using plant extracts [21, 22].

Recent study by Markova [23] have supported the formation of iron-polyphenol complex using extract of green tea where no indication was shown for the synthesis of zero valent iron. However, numerous studies have demonstrated the potential of plant extract for the synthesis of Fe0 nanoparticles, whereas clear information is yet lacking on the structural feature and composition and the role of the chemical constituents of the plant extracts in the synthesis. Characterizing the form of compounds in the plant extract and their role in the synthesis is important for optimization of the synthesis parameters and predicting the environmental behavior and efficiency in application.

In addition, designing cost effective production method of nanomaterial for environmental remediation is deemed essential due to the low market value to environmental technologies. Eco-innovation is a

* Corresponding author.
E-mail address: yirbd001@mymail.unisa.edu.au (B. Desalegn).

https://doi.org/10.1016/j.heliyon.2019.e01750
Received 2 November 2018; Received in revised form 25 February 2019; Accepted 13 May 2019

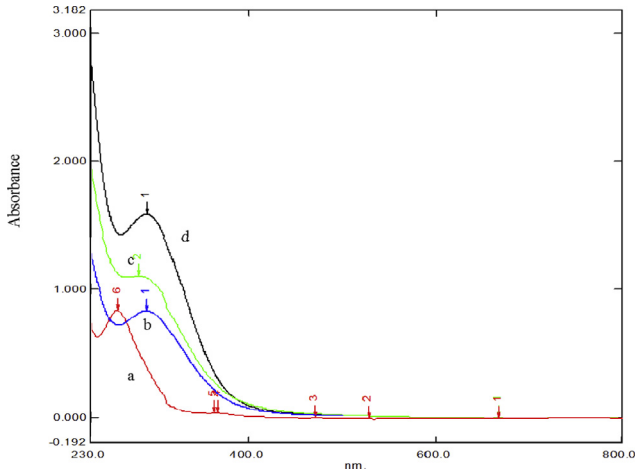

Fig. 1. Uv-vis spectra of iron nanoparticle synthesized using mango peel extract a) extract alone (b–d) increasing concentrations of the extracts.

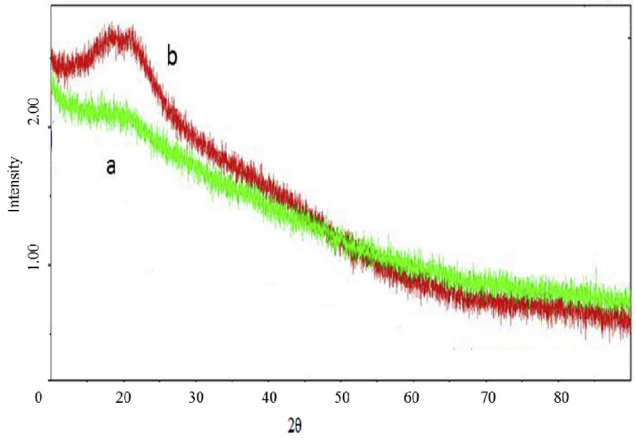

Fig. 2. XRD patterns of GMP-nZVI synthesized using mango peel extract, GMP-nZVI as-synthesized (a), after washing with methanol (b).

recent idea of technological development which considers the environmental benefits while providing low-cost production opportunity and addressing the need for sustainable technologies. Today the generation of large quantities of fruit waste has become one of the main sources of municipal solid wastes due to the high consumption and industrial processing of the parts of fruit. Due to the high global mango production and industrial demand, use of mango peel in the synthesis can be economically feasible and environmentally safe choice. The peel and stones from these processes range from 20 – 30% and 10–30% of the fresh fruit, respectively [24]. Moreover, this by-product from the industrial processing of mangoes is assumed to be 35–60% of the total fruit weight. Furthermore, studies reported higher content of polyphenols in mango peel than economically important mango flesh [25, 26, 27]. Utilization of such wastes in synthesis provides a new insight of waste recycling and nanoremediation. In this study, to synthesize nZVI (GMP-nZVI), mango peel extracts was used in the reaction medium to reduce the inorganic iron salt. Structural and compositional characteristics of GMP-nZVI were analyzed using FTIR, XPS and GC-MS. Catalytic role of GMP-nZVI was examined for the degradation of methyl orange using Fenton oxidation system.

2. Experimental

Chemicals. Iron (III) chloride hexahydrate (97%, ACS grade) and hydrogen peroxide (30%) were obtained from Sigma-Aldrich. All chemicals and solvents were used as supplied without further purification. Deionized water was used throughout the study. Commercial nZVI and nano-Fe-Ni particles were obtained from Guangzhou Jiechuang Trading Co. Ltd (Guangzhou, China) and were confirmed using X-ray diffraction (XRD). Fe3O4 nano-powder with a particle diameter <50 nm and a BET surface area of >60 m2. g-1 was purchased from Sigma-Aldrich (Castle Hill, NSW, Australia).

Biosynthesis of GMP-nZVI. The synthesis of nanozero valent iron using mango peel was briefly described in our previous work [28, 29]. We used ripened mango fruit purchased from the local market. In peeling, all flesh part was removed and was air-dried for two weeks under a shade. The air-dried peel was ground to a uniform fine powder. The extraction was performed initially by boiling one liter of water at 80 0C and adding 12 g of the fine powder and left for 12 h maintaining same temperature. The extract was centrifuged at 4,000 rpm for 10 min and filtered using Whatman paper (pore size of 25 μm). In the procedure for the synthesis of GMP-nZVI, 0.05M FeCl3•6H2O was used.. The extract was poured gradually into the aqueous solution of iron chloride. The mix was freeze dried for further analysis.

2.1. Characterization of the synthesized particle

UV-Visible spectrometer. The reduction of Fe ions to Fe° was detected by UV-Vis absorption spectroscopy (Shimadzu; UV-3600 UV-vis-NIR spectrophotometer) following dilution of freshly prepared extract and reaction mixture with MQ water. Measurement was made at a range of 200–500 nm.

EDX. The EDX spectrum was used to analyze the quantitative surface elemental profile.

X-ray diffraction (XRD). The powder sample was subjected to XRD analysis. Analyses were performed at a conditions as follows: Cu anode material, K-Alpha1 [Å] = 1.5406 with a continuous scan type operating at 40 mA and 40 kV, scanning start position [°2θ] = 10.0, scanning end position [°2θ] = 99.98, step size [°2θ] = 0.013, scan step time [s] = 148.9.

X-ray photo-electron spectroscope (XPS). Due to the iron-polyphenol complex formation (core/shell), the use of XRD might be limiting to discern the details of the particle composition on the surface and the inner structure. Thus, X-ray photo-electron spectroscope was used to reveal the elemental compositions and oxidation state of an element on the surface and internal structure of GMP-nZVI. Probing the surface chemical composition and degree of ionic characteristics was performed on Kratos Axis Ultra with DLD, equipped with a monochromatic aluminum x-ray source (E = 1486.6 eV) running at 225 W of power. The photoelectron take-off angle was at 45° to the sample surface. To avoid the shadowing effect of the ion gun at one side of the particles, electron detector was set perpendicular to the sample.

Fourier Transformed Infrared Spectroscopy (FTIR). The IR spectrum in the range of 600–4000 cm−1 of the dried mango peel extract and synthesized GMP-nZVI were recorded using Agilent Technologies, Cary 600 series FTIR Spectrometer. To increase signal to noise ratio of the spectrum, repetitive scanning was performed at a resolution of 4 cm-1 and a mirror velocity of 0.633 cm–1.

Gas chromatography-mass spectrometer (GC-MS). Compositional analysis of the extract and synthesis solution was performed using gas chromatography-mass spectrometer (GC-MS) equipped with HT5 capillary column (12 m × 0.22 mm x 0.10μm). The oven temperature was held at 25 °C for 3 min, and then increased to 300 °C at 15 °C min−1.

Degradation experiment. Methyl orange decolourization test was conducted at room temperature. Stock solution was prepared by dissolving 100 mg of the methyl orange in 1 L of deionized water. The synthesized sample (0.05 g) was mixed with 5 mL of 12% hydrogen peroxide and 30 mL of the methyl orange solution. The degradation effect was compared with few selected iron containing nanoparticles, such as bare nZVI, nano-Fe-Ni, nano-Fe3O4. Absorbance at λ-max of 465 nm was measured using UV-Visible Spectrophotometer after 1 h.

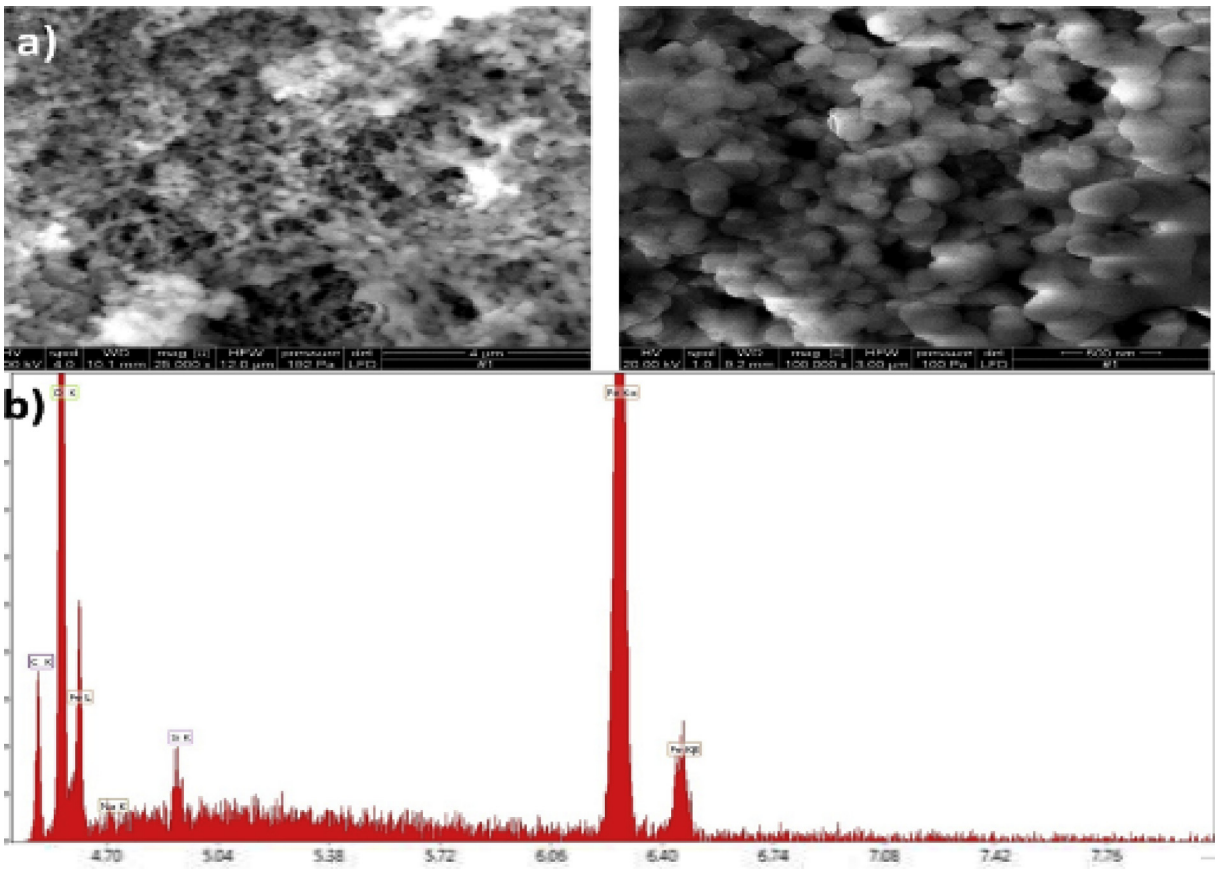

Fig. 3. EDX and Scanning-electron-micrograph (SEM) image of the GMP-nZVI a) electron image b) X-ray spectrum.

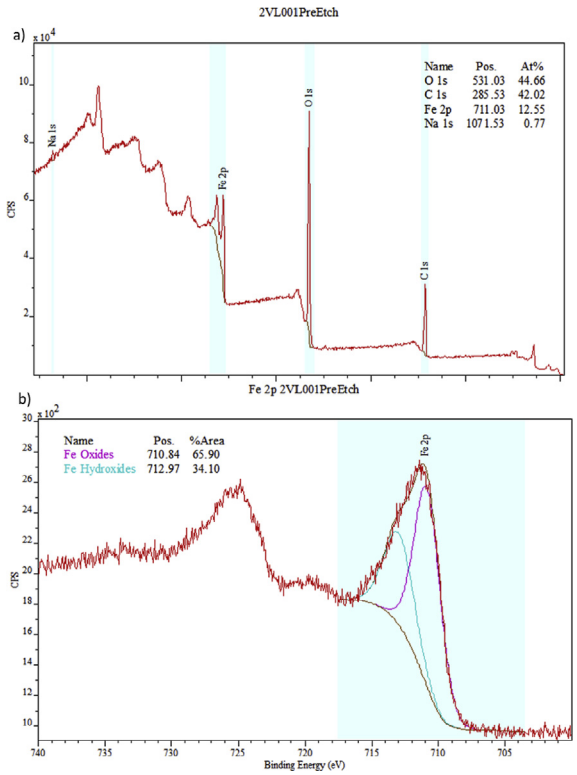

Fig. 4. Fe 2p3/2 X-ray photoelectron spectra of green synthesized nZVI; pre-etching (a and b). Shading denotes the region of binding energy for each Fe oxidation state.

Particle size of GMP-nZVI under three pH conditions and Aggregation study. Aqueous solution of ferric chloride (0.05M FeCl3•6H2O) was prepared and used for the synthesis of zerovalent iron nanoparticle under three pH conditions; i.e. 3, 6 and 9. The synthesis was carried out at room temperature with a drop-wise addition of 30 mL of a mango peel extract into a 10 mL of aqueous solution of iron chloride. For the aggregation measurement, the three soils (each 25 g) were mixed by stirring in 250 mL of water and extraction was carried out in an end-over-end shaker for 24 h. The suspended soils were centrifuged at 3,000 rpm for 20 min and the supernatant was filtered using Whatman filter paper purchased from Fisher Scientific. The stability of C-nZVI and GMP-nZVI were tested by injecting 10 mg of the nanoparticles in 30 mL of the soil extract in 40-mL clear glass vials. A 5-mL aliquot of the suspensions was taken after three days to measure the mean size and size distribution. The mean particle size, distribution of the nanoparticles in suspension was measured on Nicomp 380 ZLS Submicron Particle Sizer/Zeta Potential Analyzer (Particle Sizing Systems, Langhorne, PA, USA). Repetitive measurement was performed for each sample and mean diameter±SD values were reported.

Dissolution measurement. Dissolution of iron in the three soil solution extracts was performed by suspending 15 mg of the nanoparticles in 30 mL of the soil extract using a 40 mL glass reactor at room temperature. Aliquot were collected at interval of time (6, 12, 24, 48, 72 h). The samples were centrifuged at 3, 000 g for 10 min. The supernatant was collected and then filtered using a 0.2 μm Millipore filter. The soluble Fe concentrations in the solutions were measured in acidified solutions (0.1 MHNO3) by ICP-OES.

3. Results and discussion

Biosynthesis of GMP-nZVI. With a step-wise addition of the mango peel extract onto the iron solution, a dark brown color was observed,

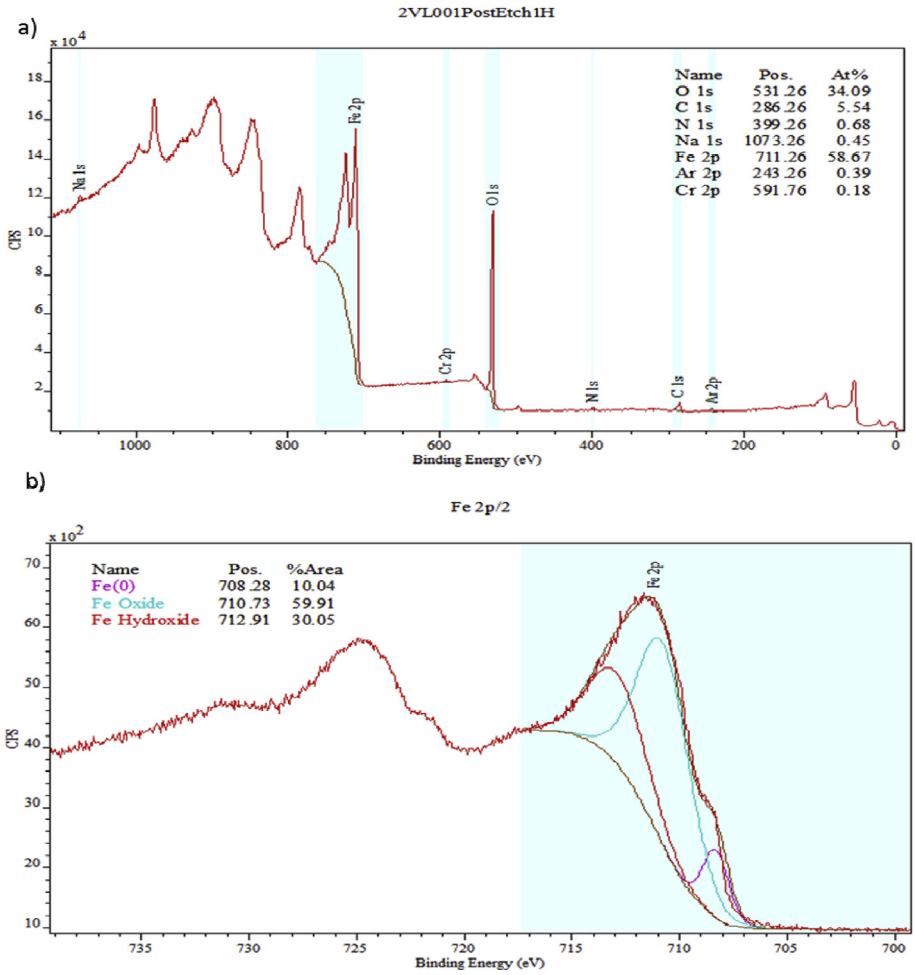

Fig. 5. Fe 2p3/2 X-ray photoelectron spectra of green synthesized nZVI, post-etching (a and b). Shading denotes the region of binding energy for each Fe oxidation state.

suggesting the formation of Fe-NPs (Fig. 1). The gradual change in the color of reaction mixture from light brown to dark brown with the addition of varying concentration of mango peel extract indicates the efficiency of mango peel extract in reducing iron [17]. Reaction was held at room temperature and the pH value of the reaction mixture was 2.1. The zeta potentials (ζ) after 3 Hr, 24 h and 3° days reaction mixture were 21.1, 18.2, and. No precipitation was observed over the period one month which could be the role of polyphenol in steric stabilization against agglomeration of Fe NP.

UV-Vis Absorption. The UV-Vis spectra for all samples have continuous absorption (Fig. 1). The mango peel extract showed visible UV spectra in the wavelength range of 200–400 nm. The surface plasmon resonance peak in the range of 250–280 nm is conforming the phenolic acid and their derivatives. The UV-Vis spectra for the synthesized GMP-nZVI under varying concentration of the extract (b = 1:1, c = 1:2 and d = 1:3 ratio of iron salt to mango peel extract) showed absorption similar to the results demonstrated by Nadagouda et'al [17] and Njagi, et'al [16]. The three reaction mixtures showed slightly varying absorption whereas the absorption for aqueous extract begins at 400 nm. The surface plasmon resonance appeared as clear peak as the concentration of mango peel extract increased in the reaction mixture. The varying UV spectra indicate the varying number of absorbing particles which could be attributable to the concentration of GMP-nZVI.

XRD. Synthesis of GMP-nZVI via chemical approach can be easily discernible using XRD analysis (Fig. 2). As shown in the XRD patterns of the synthesized iron nanoparticles, no obvious characteristic peaks were observed, confirming the absence of any ordered crystalline structure. To avoid the interference of organics, the synthesized GMP-nZVI was subjected to washing by 25% methanol. The power diffraction pattern showed little difference between the particle as-synthesized and methanol-washed particles. A broader peak at 2θ = 200 was noted in the pattern of the methanol-washed particles. This shows the amorphous nature of the particle in which the polyphenols are in complexes with iron. Likewise, the amorphous nature of the synthesized particle was reported [16, 19].

SEM/EDS analysis. SEM analysis was carried out to understand the topology of GMP-nZVI displaying the amorphous nature of the mango peel extract which appeared difficult to reveal the structural uniformity of the synthesized material. Further analysis using EDS confirmed the presence of the characteristics of elemental Fe, where the elemental analysis showed compositions of oxygen (34.06%), carbon (14.95%), and iron (48.5%) (Fig. 3). This indicated the formation of an organic layer on the surface of Fe NPs. Iron was determined from the FeKα peak at 6.4 keV. The carbon and oxygen record could possibly be elements from the proteins or organic compounds present in the mango peel extracts.

X-ray photoelectron spectroscopy. A further analysis was performed using XPS which is a powerful surface-sensitive analytical instrument to determine elemental composition and the respective ionic characteristics of GMP-nZVI. The XPS spectra of the core levels of GMP-nZVI are presented in Fig. 4. The presence of O 1s, C 1s and Fe 2p3/2 on the surface were confirmed as shown in Fig. 4a&b. The O 1s and C 1s peak at 531.03 and 285.53 eV, respectively could be assigned to the C–H and C=O bonds of the phenyl ring from proteins in the mango peel extracts [30]. This is also an indication for a potential agglomeration when

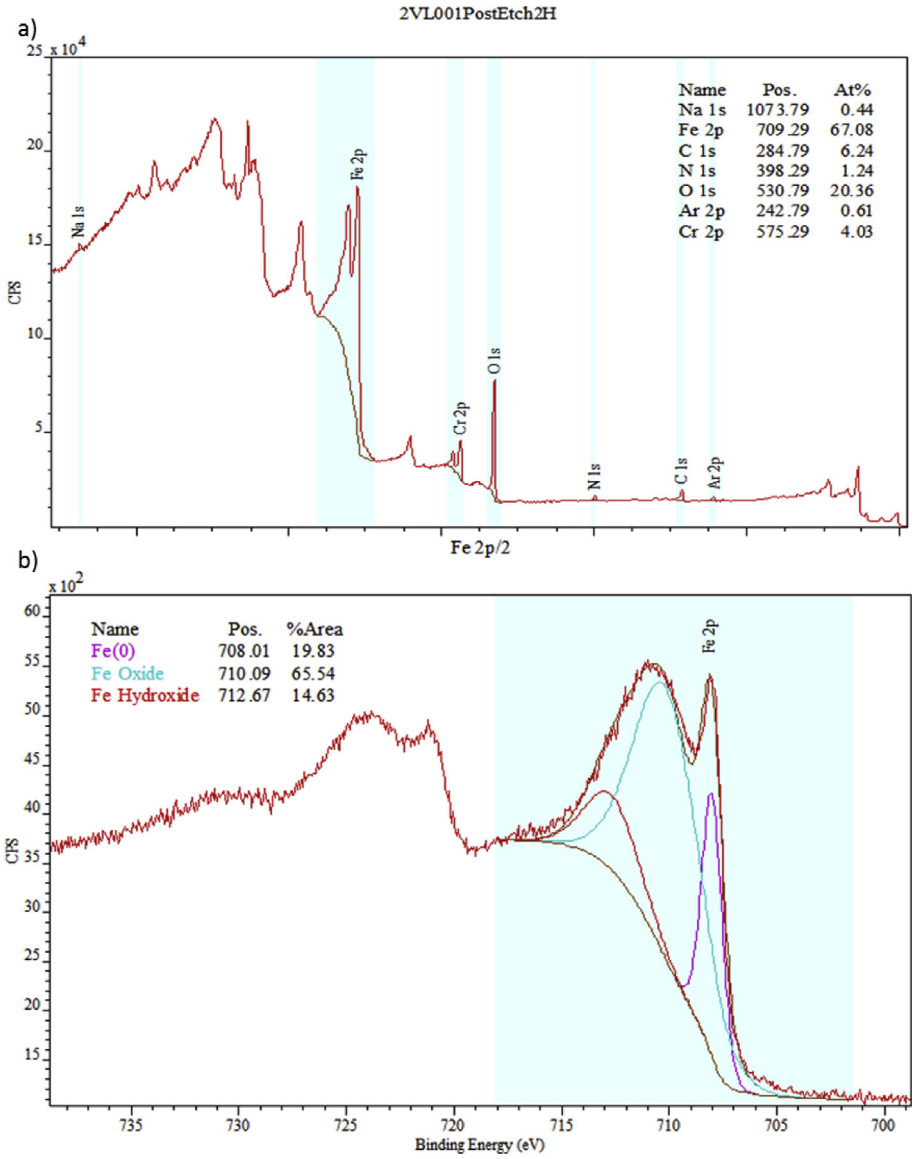

Fig. 6. X-ray photoelectron spectra showing the deep profile of the GMP-nZVI a) elemental composition b) distribution of iron form.

particles have distribution of similar size and chemistry. In addition, the high binding energy peak at position 710.84 and 712.97 eV were attributable to electron emissions from iron oxide and hydroxides. The presence of carbon implied the coating on the surface of the particle which was a limit to the detection of the absolute position of Fe0 in GMP-nZVI. The argon peak in the survey was due to the imbedded argon from the ion source.

Depth profiling of the stabilized material revealed an additional photoelectron peak at 708 eV suggest the presence of Fe0 (Fig. 5 a & b) [10, 31]. Moreover, the presence of carbon on the surface and the dramatic decreasing (a decrease by ~35%) in intensity following a slight ion etching on the sample surface indicated stabilization of GMP-nZVI. This confirms the steric stabilization of the NPs by polyphenols. The dominant peaks on the surface following the ion etching of the GMP-nZVI were observed designating the oxide and hydroxides of iron which made up 10% (Fe0), 59% (iron oxide) and 30 % (iron hydroxides) of the total iron species on the surface.

With increasing etch depth, these forms were noticed to be decreasing (from 30 % to 14% for iron hydroxides) whereas the metallic iron peak contribution increased to 20% concomitantly. The variation in oxidation state of the element with increasing etch depth could support a the model of 'Fe+3/Fe+2-polyphenol' complex islands on the metallic iron where the stabilization of Fe+3 over the Fe+2 by the polyphenol via the oxidation of the complexes of Fe+2-polyphenol to Fe+3-polyphenol occur (Fig. 6). Due to the inherently surface sensitivity of XPS to the outer 1–10 nm of the particles along with the detection of Fe0, the analysis confirmed that the shell could be less than a few nanometers thick. On the other hand, the presence of Fe0 was an indication for the state of iron ion reducing ability of mango peel extract. Moreover, the proportion of oxide layer compared to the metallic iron is a function of particle size where a small fraction of metallic iron may account for smaller particle size.

Fourier transform infrared (FTIR) analysis. Fig. 7 shows the Fourier transform infrared (FTIR) spectroscopy of the mango peel extract and synthesized GMP-nZVI to illustrate the functional groups on mango peel and predict their role in the synthesis of GMP-nZVI. Exposure to the powders in the 4000–600 cm-1 region was allowed for multiple attempts to assign the IR bands.

The spectra of GMP-nZVI and mango peel extract appeared more or less similar. Three groups of bands were observed. The broad band at 3500–3200 could be indexed to a stretching in hydrogen bonding (O–H group) of compounds such as phenol and/or carboxylic acids in pectin,

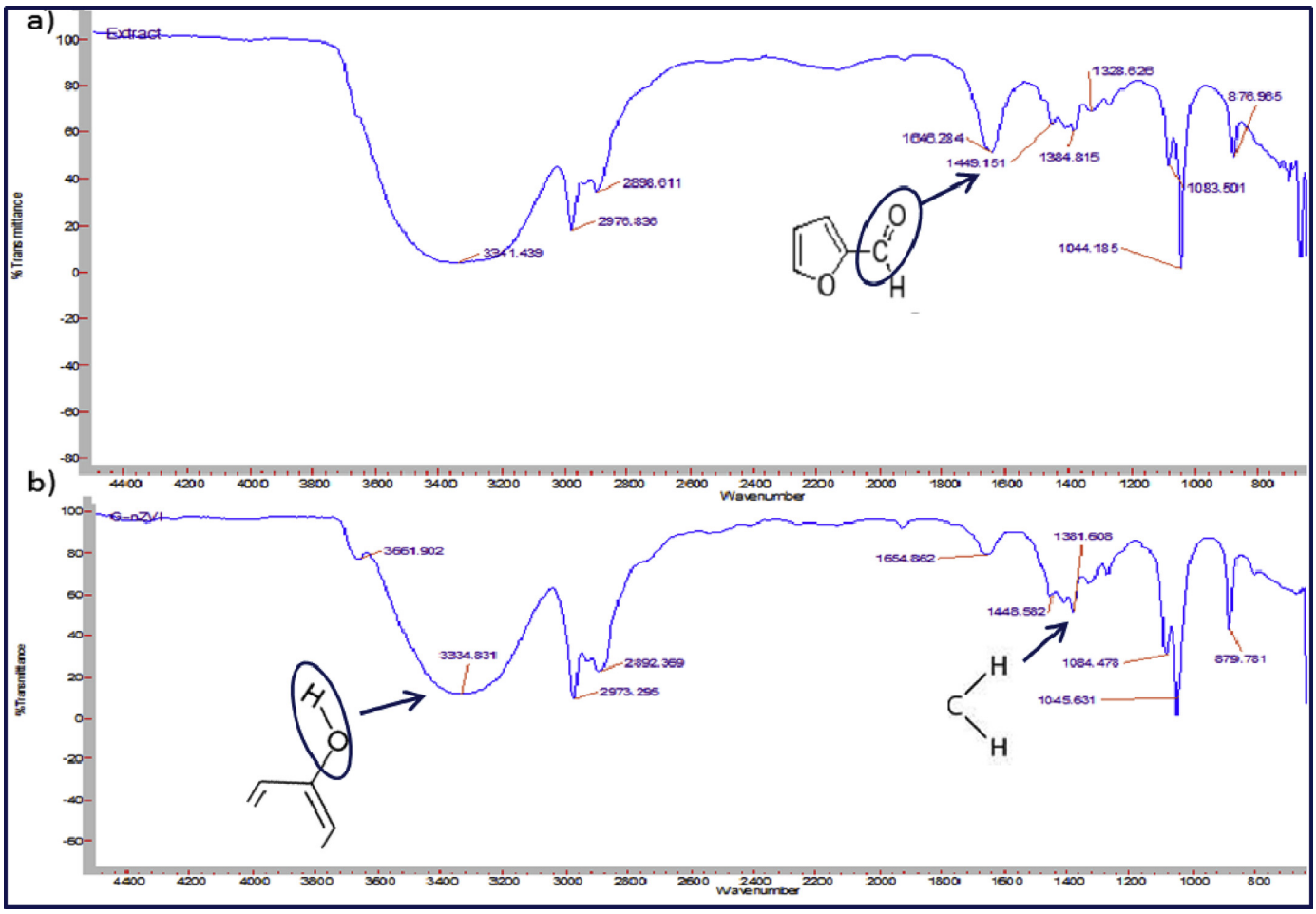

Fig. 7. FTIR spectra for a) mango peel extract and b) GMP-nZVI.

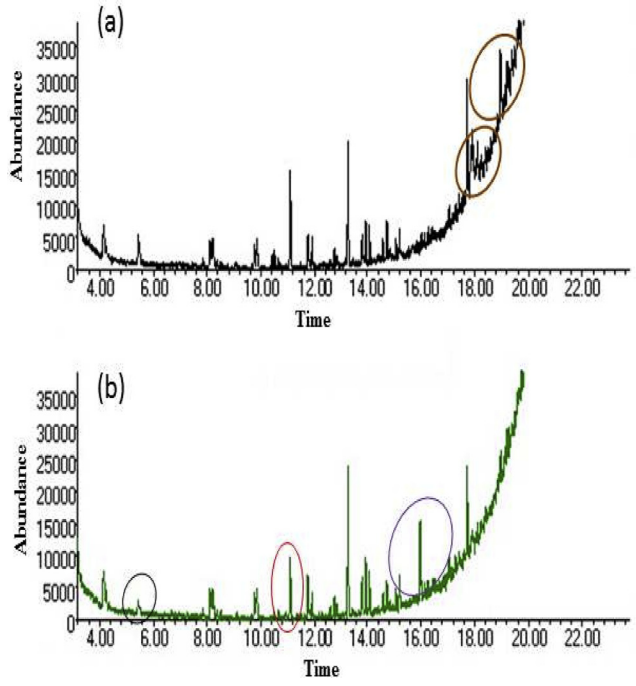

Fig. 8. Chromatogram of a) mango peel extract and b) reaction mixture (GMP-nZVI) by GC-MS analysis.

cellulose and lignin. The IR spectra of the extract and the reaction mix had somewhat similar pattern. However, the reduced intensity of the GMP-nZVI could be due to the reduction of O–H groups and the formation of iron-phenol complex. The broad range of frequencies in this band indicates the presence of free hydroxyl group [32].

For few functional groups, intensity differences and band shifts were observed, suggesting the involvement of the functional groups in reducing iron. Bands in the range of 1700 and 1600 identifies the C=O stretching vibration in aldehyde and ketones [33]. However, as shown in Fig. 7b, the absorption at band 1654 decreased and slightly shifted which could correspond to C=O stretching of amides (α-helix) from aldehyde, ketones and proteins indicating that these organic compounds may be responsible for capping. The decrease in the intensity of the band for the amides could possibly be evidence for structural change following interaction with iron particles. The bands at 1381 cm-1 could be related to the CH2 symmetric bending modes of the methyl groups of carboxylate since mango peel consists of pectin, cellulose, lignin, and flavonoid, which contain various functional groups such as aldehydes, ketone, carboxyl and hydroxyl groups [34]. The results obtained from FTIR shows that the biomolecules in the mango peel extract could be the reducing and capping agents in the green synthesis of GMP-nZVI.

Gas chromatography. Specific compositional analysis was carried out using GC-MS and compounds involved in the synthesis of GMP-nZVI were identified based on mass spectral match using manual checking in the QEdit of the MS Chemstation program (Fig. 8). Although the focus of the experiment has not been to determine the specific role of each compound in the synthesis, discussion is made to few compounds identified. Compounds such as 4H-Pyran-4-one; 2-furancarboxaldehyde

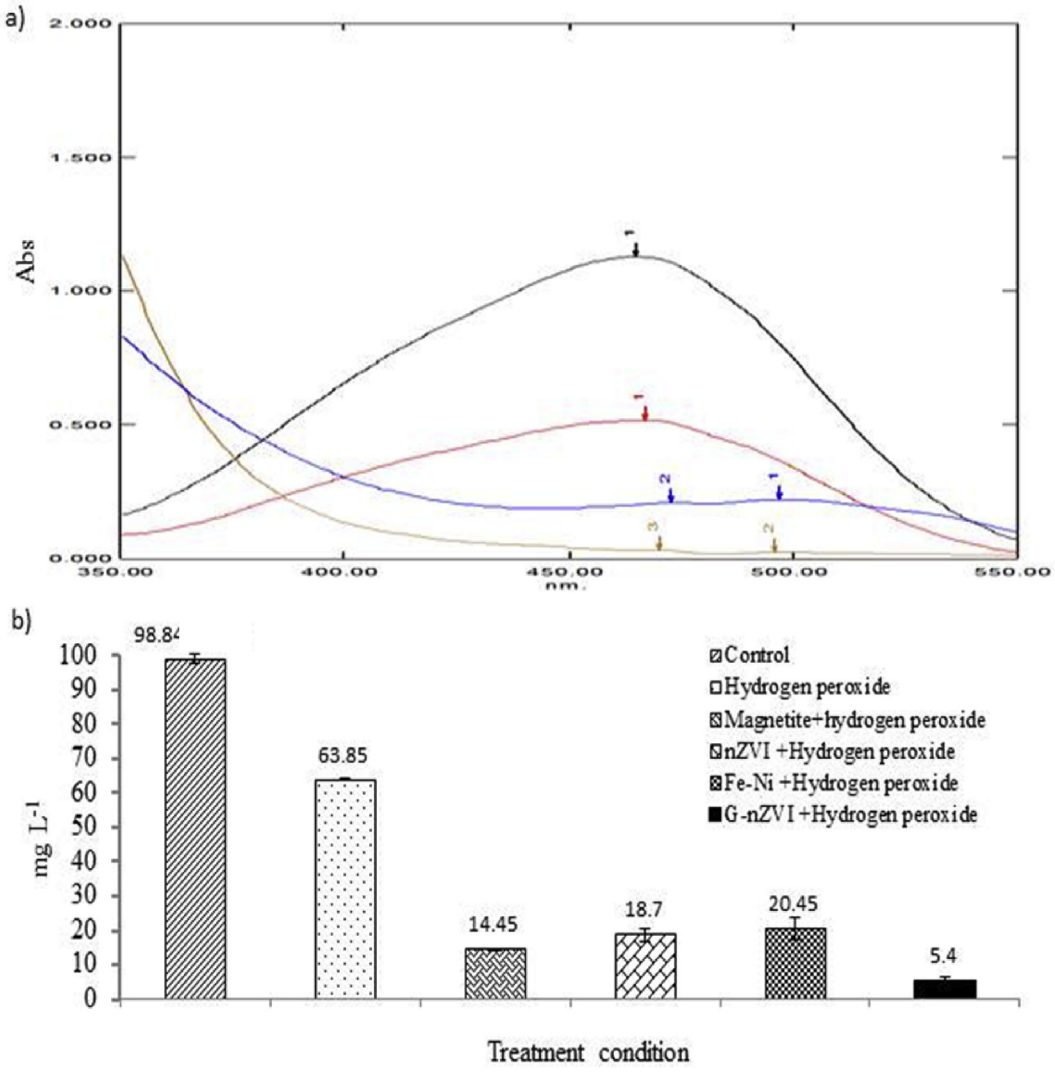

Fig. 9. Fenton oxidation of methyl orange using various catalysts including GMP-nZVI, a) absorbance of methyl orange versus wavelength b) disappearance of methyl orange under different treatment condition.

(furfural with molecular formula C5H4O2); cyclopropane-1-carboxylic acid, 5-Acetoxymethyl-2-furaldehyde, 2, 5-dihydroxyphenol; 6-Acetyl-.beta.-d-mannose and 5-hydroxymethyl-2-furancarboxaldehyde were identified. From the FTIR spectrum the broad peak at 3500 - 3200 cm−1 could be attributable to vibrations of the four –OH groups of the 4H-Pyran-4-one and 6-Acetyl-.beta.-d-mannose. As shown in Fig. 8 two peaks at a retention time of 5.471 min showed reduced intensity. According to the NIST reference, this peak is assigned to 'furfural' (Fig. 8a). From the FTIR analysis, the C=O stretching observed at 1700 and 1600 cm−1 could be from the compound 'furfural' which is the heterocyclic aldehyde group, highlighting the role of these compounds in the synthesis of GMP-nZVI. New peak at a retention time of 17.94 min was observed in the chromatogram of the reaction mix (GMP-nZVI). This is designated for cyclopropane-1-carboxylic acid (Fig. 8b).

3.1. Methyl orange degradation

Zero valent iron is readily oxidized to Fe2+ in the presence of hydrogen peroxide-an application referred to as Advanced Fenton process. The application is characterized by the solution of hydrogen peroxide and metallic iron surfaces to generate hydroxyl radicals which then oxidize recalcitrant pollutants. Particle size and their lifespan are limiting in the solution to generate Fe2+. Results from the batch experiments showed that 94.23% decolourization of the methyl orange observed. Although, this significant degradation confirmed the role of synthesized material in advanced Fenton reaction, the limit for a complete removal could possibly be a function of the initial dye concentration.

Comparison was also made for the catalytic role of the synthesized zero valent iron with the commercial forms of iron containing nanoparticles (Fig. 9). The photo-catalytic efficiency of the synthesized nZVI was by far better than the commercial nZVI, nano-Fe3O4, and nano-Fe-Ni indicating the considerably long reactive life span of the synthesized nanoparticles.

3.2. Aggregation and dissolution of GMP-nZVI in aqueous medium

The effect of pH on the particle size of nZVI during the synthesis was investigated. Particle size distributions of the three pH conditions in the synthesis of GMP-nZVI are presented in Fig. 10. Results showed that smaller and more uniform size of the nZVI particle was observed under lower pH conditions. The mean particle size at pH of 3 was 23 ± 12 nm. Whereas the particle distribution under pH conditions of 6 and 9 were with discrete peaks, indicating the role of pH in controlling the particle size of nZVI during synthesis. For example the mean particle size distributions under pH of 9 were 45 ± 4.8, 197.5 ± 28.9 and 895.8 ± 90.7 nm

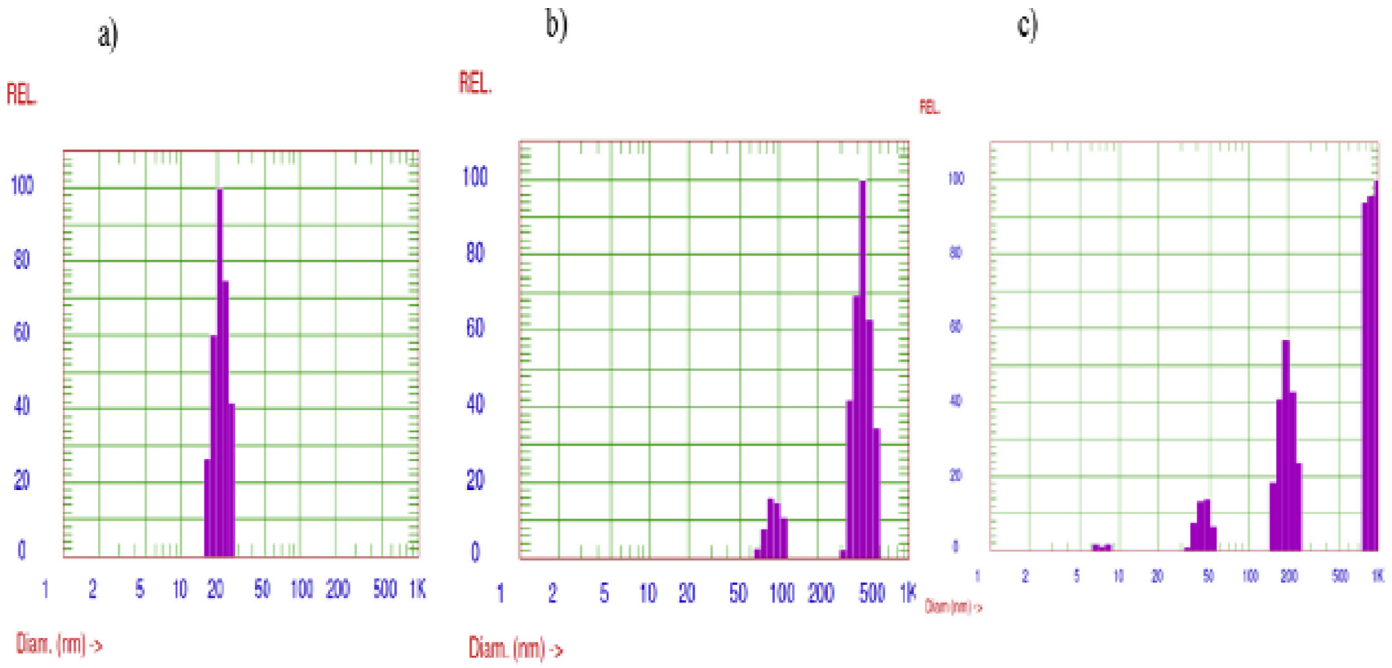

Fig. 10. Fig. 10. Particle size of GMP-nZVI under three pH condition a) pH = 3, b) pH = 6, c) pH = 9.

Fig. 11. Time dependent dissolution of GMP-nZVI treated sample in three soils.

(Fig. 10c). The nZVI synthesized using mango peel was relatively stable in the three soil suspensions. Zero valent iron in aqueous suspensions can be affected by pH, ion concentrations and charges of ions [30].

Size, crystal form, surface reactivity, surface groups and coating are characteristic for the behaviour and toxic influence of nZVI. According to the DLVO theory, size and solution ionic strength play important role on the net interaction energy between particles. The influence of ionic strengths on the aggregation of nZVI was reported pointing the chance of rapid aggregation in ground water [30]. Hence, a soil extract with less organic matter combined with the higher ionic strength (soil-3) may modify surface property and charge that can contribute for an increased agglomeration and sedimentation thereby affect reactivity.

Dissolution of GMP-nZVI was investigated. The concentration of iron in suspension was found increasing over time. As shown in Fig. 11, the dissolution rate of GMP-nZVI showed stability in soil 1 while soil 2&3 exhibited increasing pattern.

4. Conclusions

Report showing the surface characteristics and depth profile of green synthesized nZVI is scarce. This study demonstrated the synthesis of GMP-nZVI using extracts of mango peel. The synthesized material has a structure of 'Fe+3/Fe+2-polyphenol' complex islands on the metallic iron. The use of such fruit waste could be regarded as ecofriendly and economically feasible approach providing a new insight for waste recycling and nano-remediation. Understanding of the role of different polyphenol compounds in stabilizing the particle and changes in the surface characteristics and stability against desorption and biodegradation is required.

Declarations

Author contribution statement

Biruck Desalegn: Conceived and designed the experiments; Performed the experiments; Analyzed and interpreted the data; Contributed reagents, materials, analysis tools or data; Wrote the paper.

Mallavarapu Megharaj, Zuliang Chen, Ravi Naidu: Conceived and designed the experiments.

Funding statement

This work was supported by CRC/CARE, Australia.

Competing interest statement

The authors declare no conflict of interest.

Additional information

No additional information is available for this paper.

References

[1] X. Zhang, S. Lin, Z. Chen, M. Megharaj, R. Naidu, Kaolinite-supported nanoscale zero-valent iron for removal of Pb2+ from aqueous solution: reactivity, characterization and mechanism, Water Res. 45 (2011) 3481–3488.
[2] G.C. Allen, M.T. Curtis, A.J. Hooper, P.M. Tucker, X-Ray photoelectron spectroscopy of iron-oxygen systems, J. Chem. Soc., Dalton Trans. 14 (1974) 1525–1530.
[3] Z. Chen, Y. Cheng, Z. Chen, M. Megharaj, R. Naidu, Kaolin-supported nanoscale zero-valent iron for removing cationic dye–crystal violet in aqueous solution, J. Nanoparticle Res. 14 (2012) 1–8.
[4] Z. Chen, X.-y. Jin, Z. Chen, M. Megharaj, R. Naidu, Removal of methyl orange from aqueous solution using bentonite-supported nanoscale zero-valent iron, J. Colloid Interface Sci. 363 (2011) 601–607.
[5] Z. Chen, T. Wang, X. Jin, Z. Chen, M. Megharaj, R. Naidu, Multifunctional kaolinite-supported nanoscale zero-valent iron used for the adsorption and degradation of crystal violet in aqueous solution, J. Colloid Interface Sci. 398 (2013) 59–66.
[6] R.A. Crane, T.B. Scott, Nanoscale zero-valent iron: future prospects for an emerging water treatment technology, J. Hazard Mater. 211–212 (2012) 112–125.
[7] N.V. Farinella, G.D. Matos, M.A.Z. Arruda, Grape bagasse as a potential biosorbent of metals in effluent treatments, Bioresour. Technol. 98 (2007) 1940–1946.
[8] F. He, D. Zhao, Manipulating the size and dispersibility of zerovalent iron nanoparticles by use of carboxymethyl cellulose stabilizers, Environ. Sci. Technol. 41 (2007) 6216–6221.
[9] H. Kim, J.Y. Moon, H. Kim, D.-S. Lee, M. Cho, H.-K. Choi, Y.S. Kim, A. Mosaddik, S.K. Cho, Antioxidant and antiproliferative activities of mango (Mangifera indica L.) flesh and peel, Food Chem. 121 (2010) 429–436.
[10] H.-J. Kim, T. Phenrat, R.D. Tilton, G.V. Lowry, Fe0 nanoparticles remain mobile in porous media after aging due to slow desorption of polymeric surface modifiers, Environ. Sci. Technol. 43 (2009) 3824–3830.
[11] M.M. Krol, A.J. Oleniuk, C.M. Kocur, B.E. Sleep, P. Bennett, Z. Xiong, D.M. O'Carroll, A field-validated model for in situ transport of polymer-stabilized nZVI and implications for subsurface injection, Environ. Sci. Technol. 47 (2013) 7332–7340.
[12] J. Macanás, L. Ouyang, M.L. Bruening, M. Muñoz, J.C. Remigy, J.F. Lahitte, Development of polymeric hollow fiber membranes containing catalytic metal nanoparticles, Catal. Today 156 (2010) 181–186.
[13] D.E. Meyer, K. Wood, L.G. Bachas, D. Bhattacharyya, Degradation of chlorinated organics by membrane-immobilized nanosized metals, Environ. Prog. 23 (2004) 232–242.
[14] K.S. Navid Saleh, Yueqiang Liu, Tanapon Phenrat, Bruno Dufour, Krzysztof Matyjaszewski, Robert D. Tilton, Gregory V. Lowry, Surface modifications enhance nanoiron transport and NAPL targeting in saturated porous media, Environ. Eng. Sci. 24 (2007) 45–57.
[15] G.E. Hoag, J.B. Collins, J.L. Holcomb, J.R. Hoag, M.N. Nadagouda, R.S. Varma, Degradation of bromothymol blue by 'greener' nano-scale zero-valent iron synthesized using tea polyphenols, J. Mater. Chem. 19 (2009) 8671–8677.
[16] E.C. Njagi, H. Huang, L. Stafford, H. Genuino, H.M. Galindo, J.B. Collins, G.E. Hoag, S.L. Suib, Biosynthesis of iron and silver nanoparticles at room temperature using aqueous sorghum bran extracts, Langmuir 27 (2010) 264–271.
[17] M.N. Nadagouda, A.B. Castle, R.C. Murdock, S.M. Hussain, R.S. Varma, In vitro biocompatibility of nanoscale zerovalent iron particles (NZVI) synthesized using tea polyphenols, Green Chem. 12 (2010) 114–122.
[18] J.T. Nurmi, P.G. Tratnyek, V. Sarathy, D.R. Baer, J.E. Amonette, K. Pecher, C. Wang, J.C. Linehan, D.W. Matson, R.L. Penn, M.D. Driessen, Characterization and properties of metallic iron Nanoparticles: spectroscopy, electrochemistry, and kinetics, Environ. Sci. Technol. 39 (2004) 1221–1230.
[19] Z. Wang, Iron complex nanoparticles synthesized by Eucalyptus leaves, ACS Sustain. Chem. Eng. 1 (2013) 1551–1554.
[20] Z. Wang, C. Fang, M. Megharaj, Characterization of iron–polyphenol nanoparticles synthesized by three plant extracts and their Fenton oxidation of azo dye, ACS Sustain. Chem. Eng. 2 (2014) 1022–1025.
[21] N. Kataria, V.K. Garg, Green synthesis of Fe3O4 nanoparticles loaded sawdust carbon for cadmium (II) removal from water: regeneration and mechanism, Chemosphere 208 (2018) 818–828.
[22] F. Zhu, S. He, T. Liu, Effect of pH, temperature and co-existing anions on the Removal of Cr(VI) in groundwater by green synthesized nZVI/Ni, Ecotox. Tox. Environ. Safe. 15 (2018) 544–550.
[23] Z. Markova, P. Novak, J. Kaslik, P. Plachtova, M. Brazdova, D. Jancula, K.M. Siskova, L. Machala, B. Marsalek, R. Zboril, R. Varma, Iron(II,III)–Polyphenol complex nanoparticles derived from green tea with remarkable ecotoxicological impact, ACS Sustain. Chem. Eng. 2 (2014) 1674–1680.
[24] N. Berardini, R. Fezer, J. Conrad, U. Beifuss, R. Carle, A. Schieber, Screening of mango (mangifera indica L.) cultivars for their contents of flavonol O- and xanthone C-glycosides, anthocyanins, and pectin, J. Agric. Food Chem. 53 (2005) 1563–1570.
[25] R. Gnanasambandam, A. Proctor, Determination of pectin degree of esterification by diffuse reflectance Fourier transform infrared spectroscopy, Food Chem. 68 (2000) 327–332.
[26] J.A. Larrauri, P. Rupérez, B. Borroto, F. Saura-Calixto, Mango peels as a new tropical fibre: preparation and characterization, LWT – Food Sc. Techn. 29 (1996) 729–733. 25.
[27] M. Iqbal, A. Saeed, S.I. Zafar, FTIR spectrophotometry, kinetics and adsorption isotherms modeling, ion exchange, and EDX analysis for understanding the mechanism of Cd2+ and Pb2+ removal by mango peel waste, J. Hazard Mater. 164 (2009) 161–171.
[28] B.D. Yirsaw, M. Megharaj, Z. Chen, R. Naidu, Reduction of hexavalent chromium by green synthesized nano zero valent iron and process optimization using response surface methodology, Environ Tech Innov 5 (2016) 136–147.
[29] B.D. Yirsaw, M. Megharaj, Z. Chen, R. Naidu, Green mango peel-nanozerovalent iron activated persulfate oxidation of petroleum hydrocarbons in oil sludge contaminated soil, Environ Tech & Inn. 11 (2018) 142–152.
[30] T. Phenrat, N. Saleh, K. Sirk, R.D. Tilton, G.V. Lowry, Aggregation and sedimentation of aqueous nanoscale zerovalent iron dispersions, Environ. Sci. Technol. 41 (2006) 284–290.
[31] L. Sha, G. Xueyi, F. Ningchuan, T. Qinghua, Adsorption of Cu2+ and Cd2+ from aqueous solution by mercapto-acetic acid modified orange peel, Colloids Surf., B 73 (2009).
[32] P. Usha Rani, P. Rajasekharreddy, Green synthesis of silver-protein (core–shell) nanoparticles using Piper betle L. leaf extract and its ecotoxicological studies on Daphnia magna, Colloids Surf., A 389 (2011) 188–194.
[33] T. Phenrat, T.C. Long, G.V. Lowry, B. Veronesi, Partial oxidation ("Aging") and surface modification decrease the toxicity of nanosized zerovalent iron, Environ. Sci. Technol. 43 (2008) 195–200.
[34] S. Iravani, Green synthesis of metal nanoparticles using plants, Green Chem. 13 (2011) 2638–2650.